ISSN: 2692-5397
DOI: 10.33552/MCMS.2024.07.000653
Modern Concepts in Material Science
Iris Publishers

Research article



# Effect of Chlorine Doping on ZnSe Thin Films and Photovoltaic Devices

**Tamara Potlog[1]*, Ivan Gadiac[1], Noelle Gogneau[2], Lucian Pintilie[3]**

[1]*Laboratory of Organic/Inorganic Material for Optoelectronics, Moldova State University, Moldova*

[2]*Center for Nanosciences and Nanotechnologies, University of Paris-Saclay, France*

[3]*National Institute of Materials Physics, Romania*

***Corresponding author:** Tamara Potlog, Laboratory of Organic/Inorganic Material for Optoelectronics, Moldova State University, Moldova.

**Received Date:** December 09, 2024

**Published Date:** December 17, 2024

## Abstract

The nanocrystalline ZnSe thin films grown by close space sublimation (CSS) method have been optimized through chemical and thermal annealing. Nanocrystalline ZnSe films were prepared on $SnO_2$/ glass substrates at different substrates temperatures. The $SnO_2$: F film had a thickness of 500 nm, sheet resistance of <10 Ω/□. The structural, morphological and optical changes of as-deposited ZnSe thin films and after the immersion in a $ZnCl_2$:$H_2O$ solution and annealing at 400°C, for 30 minutes, were studied by XRD, SEM, EDS, UV-Vis techniques. The SEM and XRD investigation of as-deposited ZnSe thin films show that films are polycrystalline and have the cubic zincblende structure. The nanograin sizes and the lattice parameters of ZnSe thin films depend on the substrate temperature. After the chemical doping and annealing, the EDS spectra of the immersed ZnSe films show the presence of chlorine in the films. Both, as-deposited ZnSe thin films and annealed, were Zn deficient. The transmittance and energy band gap of nanocrystalline ZnSe films decrease after$ZnCl_2$:$H_2O$ doping and annealing. The ZnSe/CdTe photovoltaic cells were characterized through light and dark current density–voltage (J–V) measurements. The photovoltaic parameters of ZnSe/CdTe thin film solar cells improved after the immersion in a solution of $ZnCl_2$:$H_2O$ and annealing at 400°C. The best photovoltaic parameters of the ZnSe/CdTe device reached $V_{oc}$ = 750 mV, *FF* = 43%, $J_{sc}$ = 20.39 mA/cm$^2$, and $\eta$ =6.6 %.

**Keywords:** ZnSe thin films; $ZnCl_2$ activation; ZnSe/CdTe thin film solar cells

## Introduction

The compound semiconductor ZnSe is a promising n-type material of II-VI group with wide direct band gap (2.67 eV) and has zinc blend (cubic phase) and wurtzite (hexagonal phase) structures or the mixture of both, which depend on the deposition methods and technological conditions [1-6]. More progress has been achieved in fabrication of blue-green light emitting diodes [7,8], dielectric mirrors [9], filters [10], blue laser diode [11] and other optically sensitive devices [12]. There are a number of reports on the different structural, optical and electrical properties of ZnSe polycrystalline thin films prepared by various techniques, such as chemical vapour deposition [13], metal organic chemical vapor deposition (MOCVD) technique [14], electrodeposition [15], photochemical deposition [16], chemical bath deposition (CBD) [17], pulsed laser deposition [18] and thermal evaporation [19]. The close space sublimation (CSS) method is considered one of the most promising techniques

for A2B6 thin film deposition [20, 21]. Because of its large band gap, ZnSe has been used as window layer for the fabrication of photovoltaic solar cells. The use of ZnSe films as a heterojunction partner in II-VI thin-film solar cells has been explored by T. L. Chu at al. [22]. Therefore we have prepared the ZnSe thin films of different thicknesses by close space sublimation method at different substrate temperatures. In this paper, the different structural and optical parameters of as-deposited ZnSe thin films were estimated in dependence of the substrate temperature and after the immersion in a $ZnCl_2$:$H_2O$ solution and annealing. As absorbent, CdTe is recognized as promising absorbent for thin-film photovoltaic devices because of their near optimum direct band gap of ~1.5 eV and higher absorption coefficient. In this paper, we will study ZnSe/CdTe thin film solar cells based on doped ZnSe thin films by immersioninZn-$Cl_2$:$H_2O$ solution and annealing.

## Experimental Procedure

ZnSe films were deposited by close space sublimation technique. ZnSe and CdTe of 99.999% purity were used as source materials. The ZnSe thin films were deposited at a system pressure of $10_{-6}$ Torr on glass substrate covered with $SnO_2$. The thickness of $SnO_2$ films, with a sheet resistance of 10 Ω/square, were about 500 nm. In order, to optimize the growth parameters, ZnSe thin films were deposited at different substrate temperatures. The substrate temperature was varied rom 500 K to 650 K. Then the ZnSe films was immersed in $ZnCl_2$:$H_2O$ solution and annealed in the vacuum at 400°C, for 40 min. The ZnSe/CdTe thin-film photovoltaic heterojunctions were fabricated on glass substrates covered with a $SnO_2$ layer with an area of 2×2 $cm^2$. We used the optimized component films to fabricate ZnSe/CdTe thin-film solar cells. The ZnSe/CdTe thin-film solar cells were fabricated in a superstrate configuration. The samples with as-grown ZnSe thin films obtained at substrate temperatures 500 K, 550 K, 600 K and 650 K denoted as (M5.1), (M6.1), (M7.1) and (M8.1), respectively. The samples with ZnSe thin films activated in$ZnCl_2$:$H_2O$ solution obtained at the same substrate temperatures were signed as (M5.2), (M6.2), (M7.2),(M8.2), respectively.

The structure of ZnSe films were performed with a Rigaku X-Ray Diffractometer (XRD) with CuKα1/40 kV/40 mA radiation source (λ=1.54056 Å), Ni filter, in the 2θ range of 10°- 90°, scanning speed of 0.5°/min. The XRD analysis was performed using Rigaku software PDXL. The energy dispersive spectroscopy (EDS) analysis of the samples was performed with a JEOL JSM-6390LV scanning electron microscope. The optical transmission spectra were recorded using a JASCO V-670 spectrophotometer. The photovoltaic characteristics of ZnSe/CdTe thin film solar cells were investigated by current-voltage characteristic through the wide band gap components at the room temperature (300 K) and 100 mW/$cm^2$ illumination.

## Structural and Optical Properties of CSS Nanostructured ZnSe Thin Films

The requirements for window layers in solar cells applications are high conductivity and adequate thickness in order to allow good transmission and uniformity which would avoid the effects of short cutting. Figure 1 shows the SEM image of as-grown and after $ZnCl_2$ annealing of ZnSe films deposited on $SnO_2$/glass substrates. From the SEM image it is clear that the ZnSe films are dense and pinhole free. The grain size is smaller than 1μm in both cases. Sample M5.2 with ZnSe after $ZnCl_2$ activation at 400°C shows a lot of round grains on the surface, and they did not coalesce together. The film lost compactness of the structure. No significant changes in morphology of the M6.2 and M7.2 samples, after activation in $ZnCl_2$:$H_2O$ solution and annealing, were occurred.

Figure 2 shows XRD 2θ scans, between 20° and 80°, for ZnSe/$SnO_2$/glass samples before and after ZnCl2 activation. As seen, the XRD pattern exhibits intensive XRD peaks at 26.52°, 33.79°, 37.85°, 38.84, 42.55, 51.64, 54.51, 61.69, 71.04, 78.44 and 52° which are due to the X-ray diffraction from polycrystalline $SnO_2$ with tetragonal or orthorhombic structures [23]and four peaks with the smaller intensity for ZnSe phase presented in the Figure 2. The X-ray diffraction measurements on the as-deposited films and $ZnCl_2$ treated revealed, for both, a cubic ZnSe phase. The ZnSe phase for all samples corresponds to the 216: F- 3m space group. There is no evidence of formation of a new phase after $ZnCl_2$ annealing. The crystallite size was calculated using the Scherrer's formula [10] from the full-width at half-maximum (FWHM) $(\beta)$:

$$D = \frac{k\lambda}{\beta \cos\theta} \qquad (1)$$

Where $\lambda$ is the X-ray wavelength, θ the diffraction angle, and k a constant usually equal to 1. The micro strain $(\varepsilon)$ was calculated from formula

$$\varepsilon = \beta \cos\theta/4 \qquad (2)$$

where $\beta$ the full-width at half-maximum.

**Table 1:** Structural parameters of as-grown ZnSe thin films obtained at different substrate temperatures ($T_s$) and after $ZnCl_2$ activation.

| Samples | a(Å) | b(Å) | c(Å) | D, crystallite size (Å) | Strain (%) | Phase name |
|---|---|---|---|---|---|---|
| M51 as grown Ts=500 K | 5.6707 | 5.6707 | 5.6707 | 280 | 0.10 | Stilleite, syn |
| | 4.7502 | 4.7502 | 3.1932 | 635 | 0.15 | Cassiterite |
| M52 $ZnCl_2$_activated Ts=500 K | 4.7517 | 4.7517 | 3.1934 | 644 | 0.15 | tin(IV) oxide |
| | 5.6695 | 5.6695 | 5.6695 | 288 | 0.0001 | Stilleite, syn |

| | | | | | | |
|---|---|---|---|---|---|---|
| M61 as grown Ts=550 K | 4.7365 | 4.7365 | 3.1881 | 579 | 0.20 | tin(IV) oxide |
| | 5.6572 | 5.6572 | 5.6572 | 317 | 0.16 | Stilleite, syn |
| M62 $ZnCl_2$-activated Ts=550 K | 5.6665 | 5.6665 | 5.6665 | 314 | 0.12 | Stilleite, syn |
| | 4.7391 | 4.7391 | 3.1905 | 583 | 0.20 | tin(IV) oxide |
| M72 as grown Ts=600 K | 5.6571 | 5.6572 | 5.6571 | 337 | 0.23 | Stilleite, syn |
| | 4.7392 | 4.7392 | 3.1871 | 647 | 0.21 | tin(IV) oxide |
| M71 $ZnCl_2$-activated Ts=600 K | 4.7383 | 4.7383 | 3.1952 | 588 | 0.20 | tin(IV) oxide |
| | 5.6663 | 5.6663 | 5.6663 | 287 | 0.13 | Stilleite, syn |

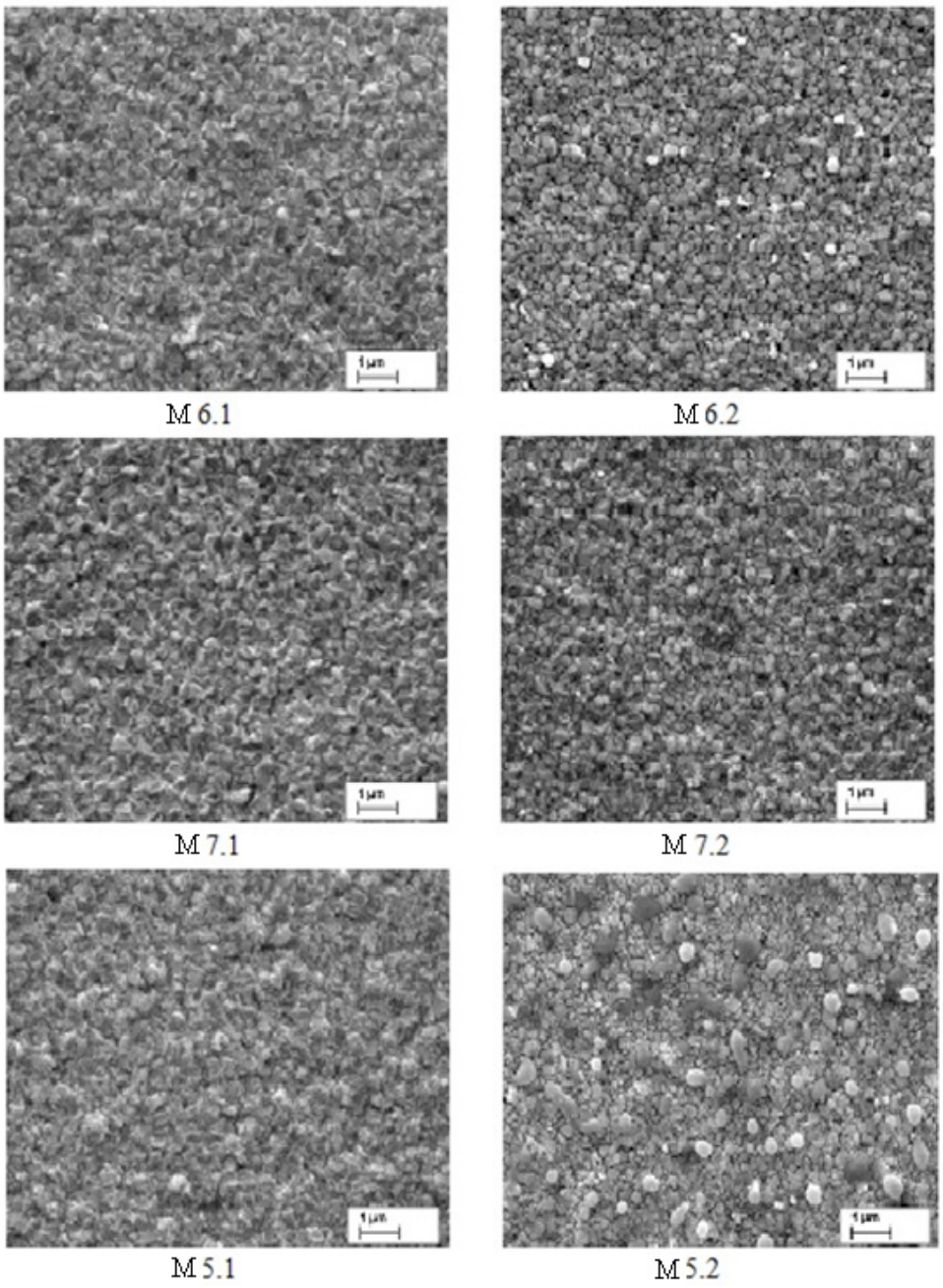


**Figure 1:** SEM images of ZnSe films: M5.1, M6.1, M7.1 – as grown; M5.2, M6.2, M7.2 – after $ZnCl_2$ activation.

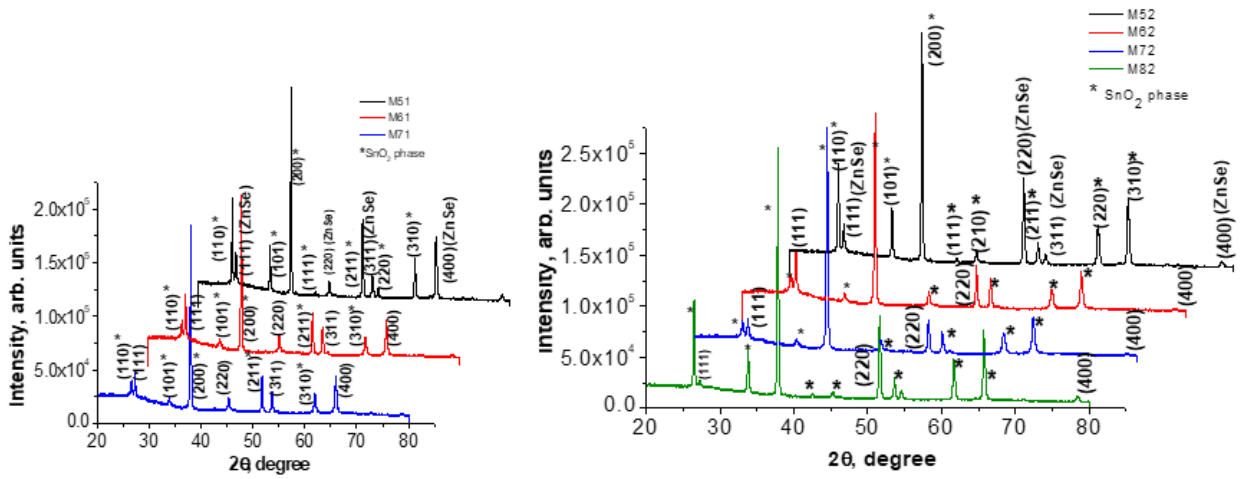


**Figure 2:** X-ray diffraction patterns of as grown (left) and after $ZnCl_2$ activation (right) ZnSe thin films at different substrate temperatures.

As shown in Table 1, the ZnSe grains are smaller than those of $SnO_2$. For both, as-grown and activated ZnSe thin films, a slight lattice-parameter decrease is revealed with varying substrate temperature. In Figure 3 is presented EDS analysis of as-deposited and annealed ZnSe thin films obtained at Ts=600 K. The data for the other substrate temperatures are not shown as they all show very similar characteristics. Both, the as-deposited and annealed ZnSe films are Zn-deficient and agree well with as reported by other authors [24]. This is because the vapor pressure of Se is greater than that of Zn and their sticking coefficients are also different. The incorporation of chlorine in the activated ZnSe layers at substrate temperatures is confirmed by the detection of chlorine in a standardizes EDS analysis.

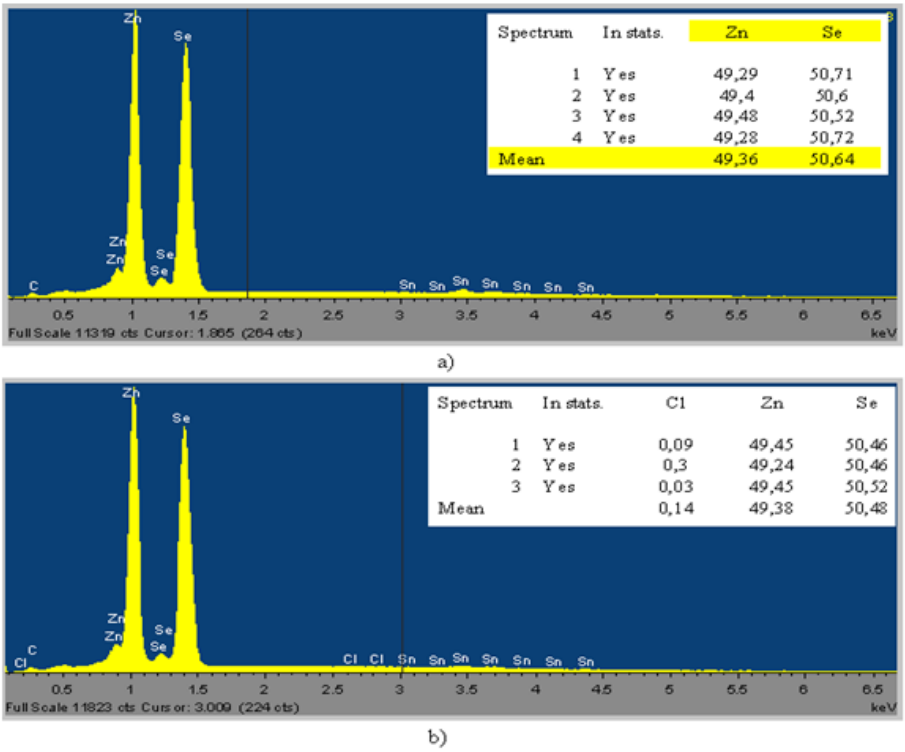


**Figure 3:** The EDX analyses of as-grown (a) and after $ZnCl_2$ activation (b) ZnSe thin films depos.

The optical transmission spectra of as deposited ZnSe thin films grown at different substrate temperatures were measured in the range of 400–1200 nm at T=300 K and shown in Figure 4. The transmission slightly changes with the substrate temperature increase. The transmittance of the layers varies between 70% - 90%, maximum of 90% being reached for ZnSe layer with a lower thickness – 236.8 Å. For ZnSe chlorine activated films transmittance is smaller. The absorption coefficient, α, was calculated from expression

$$\alpha = \frac{1}{d}\ln\frac{(1-R)^2}{T} \quad (3)$$

where $d$ is the film thickness, $R$ and $T$ are the reflection and transmission coefficient, respectively. The thickness of the ZnSe layers was estimated using the following relation:

$$d = \frac{\lambda_1\lambda_2}{2(\lambda_1 n_2 - \lambda_2 n_1)} \quad (4)$$

where $n_1$, and $n_2$ are the refractive indexes at two adjacent maxima (or minima) and $\lambda_1, \lambda_2$ the respective wavelength values. The analysis of the $(\alpha h\nu)^2 = f(h\nu)$ plot of all ZnSe films is linear and it indicates a direct type of transition. The optical band gap values for as-deposited ZnSe films fluctuated between 2.68 eV (0.63 μm) and 2.69 eV (1.16 μm). The maximum value of $E_g$ is connected with the very small size of crystallites in films. The thick films have a lower absorption value at the forbidden gap region of the ZnSe films. Thinner films have a high absorption value in the band-band absorption region. This effect may be explained by proposing that thicker films have bigger crystallites (grains) so they are closer to the crystalline ZnSe, but bigger grain sizes give results in larger unfilled inter-granular volumes so the absorption per unit thickness is reduced. One obvious result from the $(\alpha h\nu)^2 = f(h\nu)$ dependence (Figure 5) for ZnSe films grown at different substrate temperatures and $ZnCl_2$ activated at 400°C is that the energy gap decreases. The size of crystallites increases with the increase of the substrate temperatures and with $ZnCl_2$ activation. This is confirmed by the XRD analysis (Table I) and is valid for all ZnSe films regardless of the substrate temperature.

**Table 2:** The optical parameters of as-grown and $ZnCl_2$ activated ZnSe thin films.

| Samples | $\lambda_1$ | $\lambda_2$ | $n_1$ | $n_2$ | d, nm | $E_g$, eV | $T_s$ K |
|---|---|---|---|---|---|---|---|
| M5.1 | 855 | 1003 | 2,511 | 2,488 | 1159,10 | 2,6901 | 500 as-grown |
| M5.2 | 908 | 1076 | 2,502 | 2,481 | 1167,07 | 2,6673 | 500 annealed |
| M6.1 | 914 | 1288 | 2,501 | 2,466 | 633,72 | 2,6867 | 550 as-grown |
| M6.2 | 1091 | 1422 | 2,479 | 2,46 | 948,98 | 2,6721 | 550 annealed |
| M7.1 | 999 | 1422 | 2,489 | 2,46 | 678,59 | 2,6831 | 600 as-grown |
| M7.2 | 937 | 1408 | 2,497 | 2,46 | 565,07 | 2,6684 | 600 annealed |
| M8.2 | 846 | 1000 | 2,513 | 2,489 | 1098,26 | 2,6405 | 650 annealed |

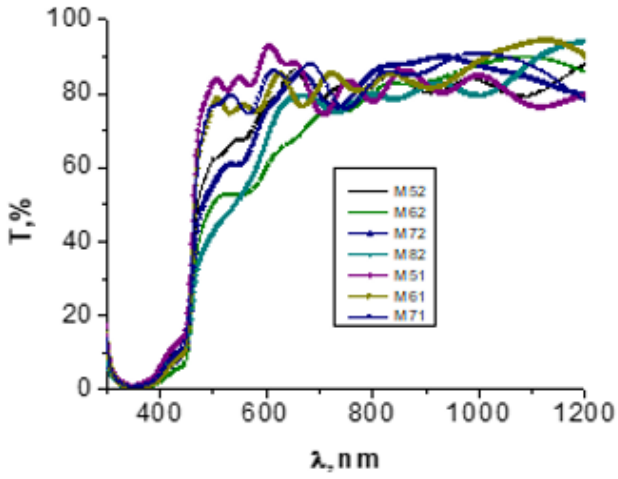


**Figure 4:** The transmission spectra of as–grown (M5.1, M6.1, M7.1) and $ZnCl_2$ activated ZnSe thin films at different substrate temperatures.

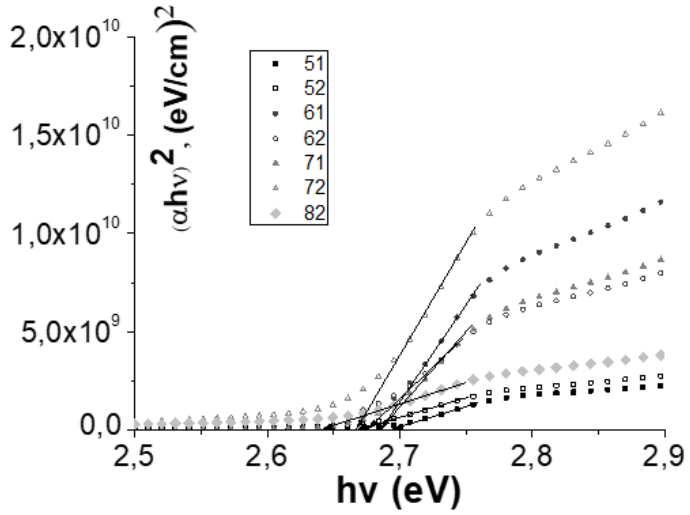


**Figure 5:** The $(\alpha h\nu)^2 = f(h\nu)$ spectra of as grown (M5.1, M6.1, M7.1) and $ZnCl_2$ activated ZnSe thin films at different substrate temperatures.

## Photovoltaic Parameters of ZnSe/CdTe Thin Film Solar Cells

The photovoltaic characteristics of ZnSe/CdTe thin film solar cells were investigated through the wide band gap component at the room temperature (300 K) and 100 mW/cm$^2$ illumination. The current density-voltage (J-V) characteristics of ZnSe/CdTe thin film solar cells with ZnSe activated at different substrate temperatures are illustrated in Figure 6. The photovoltaic parameters are presented in Table 3. The highest efficiency 6.6 % was achieved for ZnSe/CdTe thin film solar cells with a thicker ZnSe activated buffer layer.

**Table 3:** Photovoltaic parameters of ZnSe/CdTe solar cells.

| | $T_s$, K | $J_{sc}$, mA/cm$^2$ | $U_{oc}$, V | FF | η,% | $R_{sh}$, Ω·cm$^2$ | $R_s$, Ω·cm$^2$ |
|---|---|---|---|---|---|---|---|
| M8.2 | 650 | 18.45 | 0.78 | 0.37 | 5.34 | 168.62 | 23.66 |
| M7.2 | 600 | 10.70 | 0.74 | 0.42 | 3.30 | 333.33 | 30.30 |
| M6.2 | 550 | 12.13 | 0.73 | 0.39 | 3.46 | 176.08 | 34.04 |
| M5.2 | 500 | 20.39 | 0.75 | 0.43 | 6.61 | 380.00 | 17.02 |

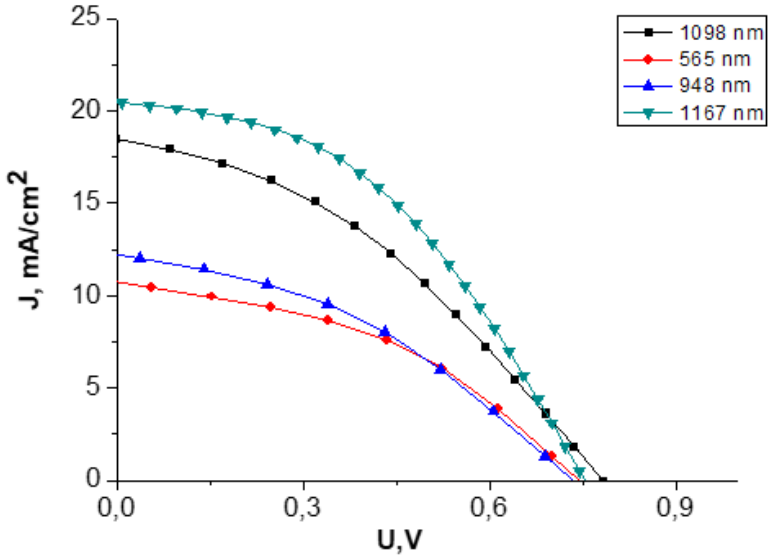


**Figure 6:** The current density-voltage (J-V) characteristics of ZnSe/CdTe thin film solar cells with ZnSe activated at different substrate temperatures.

As one can see from Table 3 the value of the open circuit voltage ($U_{oc}$) and the current density ($J_{sc}$) achieve 0.75 V and 20.39 mA/cm$^2$, respectively. The fill factor (*FF*) is low in general. According to the theory [19] the fill factor is determined by the series resistance, the saturated dark current density ($J_o$) and the diode quality factor (A). The dark Jo and A of the ZnSe/CdTe cells are in the range of $10^{-9}$ – $10^{-7}$ A/cm$^2$ and 1.7-3.6, respectively. The low value of *FF* is mainly determined by the high value of the series resistance which is due to the high resistivity of both ZnSe and CdTe thin films and probably to the fact that the cells wet $CdCl_2$ treatment may contain oxide on the surface of CdTe.

## Conclusion

In situ $ZnCl_2$ activation promotes the increasing of the crystallite's sizes and improvement of the photovoltaic parameters in ZnSe/CdTe thin film solar cells. Also, with the increasing of the substrate temperature the crystallites sizes increase from 280 nm (500 K) to 337 nm (600 K). The analysis of the XRD spectra of the both, as-deposited and annealed ZnSe thin films, established a slight lattice-parameter decrease. The EDS analysis showed that the as-grown and annealed ZnSe films are Zn-deficient. In the activated ZnSe thin films, the presence of chlorine was depicted. The transmission and the band gap energy of the $ZnCl_2$ activated ZnSe thin films decrease. The efficiency of 6.6 % for ZnSe/CdTe thin film solar cells with a ZnSe activated window layer was achieved.

## Acknowledgement

This publication is based upon work from COST Action OPERA – European Network for Innovative and Advanced Epitaxy – CA20116, supported by COST (European Cooperation in Science and Technology, www.cost.eu).

## Conflict of Interest

None.

## References

1. Venkatachalam S, Agilan S, Mangalaraj D, Narayandass Sa K (2007) Optoelectronic properties of ZnSe thin films. Mat Sci Semicon Proc 10(2-3): 128-132.
2. Kumaresan R, Ichimura M, Arai E (2002) Photochemical Deposition of ZnSe Polycrystalline Thin Films and Their Characterization, Thin Solid Films 414(1): 25-30.
3. Lokhande C D, Patil P S, Tributsch H, Ennaoui A (1998) ZnSe thin films by chemical bath deposition method. Solar Energy Materials and Solar Cells 55(4): 379-393.
4. R B Kale, CD Lokhande (2005) Influence of air annealing on the structural, morphological, optical and electrical properties of chemically deposited ZnSe thin films. Appl Surface Science 252(4): 929-938.
5. Liangyan Chen, Daoli Zhang,Guangmei Zhai, Jianbing Zhang (2010) Comparative study of ZnSe thin films deposited from modified chemical bath solutions with ammonia-containing and ammonia-free precursors. Materials Chemistry and Physics 120(2-3): 456-460.
6. G Perna, M Lastella, M Ambrico, V Capozzi (2006) Temperature dependence of the optical properties of ZnSe films deposited on quartz substrate. Appl Physics A 83(1): 127-130.
7. M W Cho, J H Chang, H Wenisch Yao (2000) Blue-Green Light Emitting Diodes with New p-Contact Layers: ZnSe/BeTe. Phys Stat Solidi (a) 180(1): 217-223.
8. M A Haase, J Qiu, J D DeP, H Cheng (1991) Blue-Green Laser Diodes. Applied Physics Letters 59: 1272-1274.
9. Z Nasiri, H Fallah, M Hajimahmoodzadeh, M Mardiha (2021) Investigation of the laser induced damage thresholds of all-dielectric and metal-dielectric mirrors for a continuous wave at 10.6μm. Optical Materials 114: 110936.
10. G R Olbright, N Peyghambarian, H M Gibbs, H A Macleod, F Van Milligen, et al. (1984) Microsecond room-temperature optical bistability and crosstalk studies in ZnS and ZnSe interference filters with visible light and milliwatt powers. Appl Phys Lett 45: 1031-1033.
11. Gokhale, Milind R (1995) OMVPE growth and characterization of ZnSe based materials for blue-green laser applications. Doctoral Dissertations pp. AAI9605510.
12. Shimizu A, Chaisitsak S, Sugiyama T, Yamada A, Kongai M, et al. (2002) Zinc-based buffer layer in the Cu(InGa)Se2 thin film solar cells. Thin Solid Films 361-362: 193-197.
13. CD Lokhande, PS Patil, H Tributsch, A Ennaoui (1998) ZnSe thin films by chemical bath deposition method. Solar Energy Materials and Solar Cells 55(4): 379-393.
14. T Aoki, M Morita, S Wickramanayaka, Y Nakanishi, Y Hatanaka, et al. (1996) Growth of ZnSe thin films by radical assisted MOCVD method. Applied Surface Science 92: 132-137.
15. Xu JL, Gong WY, Wang W, Hao Meng, Xia Zhang, et al. (2017) Electrodeposition mechanism of ZnSe thin film in aqueous solution. Rare Met 36: 816-820.
16. G Hodes (1995) Physical electrochemistry: Principles, Methods and Applications. Marcel Dekker Inc. New York pp. 515-554.
17. Sagadevan S, Das I (2016) Chemical bath deposition (CBD) of zinc selenide (ZnSe) thin films and characterisation. Australian Journal of Mechanical Engineering 15(3): 222-227.
18. G Perna, V Capozzi, MC Plantamuraa, A Minafra, P F Biag, et al. (2002) Structural and optical properties of pulsed laser-deposited ZnSe flims. Applied Surface Science 186(1-2): 521-526.
19. J E Bernard, A Zunger (1987) Electronic Structure of ZnS, ZnSe, ZnTe and their Pseudobinary Alloys. Physical Review 36(6): 3199-3228.
20. S Armstrong, PK Datta, RW Miles (2002) Properties of Zinc Sulphur Selenide Deposited using a Close-Spaced Sublimation Method. Thin Solid Films 403-404: 126-129.
21. S Armstrong, PK Datta, RW Miles (2002) Properties of Zinc Sulphur Selenide Deposited using a Close-Spaced Sublimation Method. Thin Solid Films 403-404: 126-129.
22. T L Chu, Shirley S Chu, G Chen, J Britt, C Ferekides, et al. (1992) Zinc selenide films and heterojunctions. J Appl Phys 71: 3865-3869.
23. JCPDS X-ray powder files data (Data file 05–0522).
24. RW Miles (2002) Properties of Zinc Sulphur Selenide Deposited using a Close-Spaced Sublimation Method. Thin Solid Films 403-404: 126-129.